IOP Publishing Journal of Physics: Condensed Matter
J. Phys.: Condens. Matter **32** (2020) 155401 (9pp) https://doi.org/10.1088/1361-648X/ab62bf

An all-atom kinetic Monte Carlo model for chemical vapor deposition growth of graphene on Cu(1 1 1) substrate

Shuai Chen[1], Junfeng Gao[2], Bharathi M Srinivasan[1], Gang Zhang[1], Viacheslav Sorkin[1], Ramanarayan Hariharaputran[1] and Yong-Wei Zhang[1,3]

[1] Institute of High Performance Computing, A*STAR, 138632, Singapore
[2] Key Laboratory of Materials Modification by Laser, Ion and Electron Beams, Dalian University of Technology, Ministry of Education, Dalian 116024, People's Republic of China

E-mail: zhangyw@ihpc.a-star.edu.sg

Received 5 November 2019, revised 24 November 2019
Accepted for publication 17 December 2019
Published 10 January 2020

Abstract

Various graphene morphologies (compact hexagonal, dendritic, and circular domains) have been observed during chemical vapor deposition (CVD) growth on Cu substrate. The existing all-atom kinetic Monte Carlo (kMC) models, however, are unable to reproduce all these graphene morphologies, suggesting that some crucial atomistic events that dictate the morphology are missing. In this work, we propose an all-atom kMC model to simulate the graphene CVD growth on Cu substrate. Besides the usual atomistic events, such as the deposition and diffusion of carbon species on the substrate, and their attachments to the edge, we further include three other important events, that is, the edge attachment of carbon species to form a kink, the diffusion of carbon species along the edge, and the rotation of dimers to form kinks. All the energetic parameters of these events are obtained from first-principles calculations. With this new model, we successfully predict the growth of various graphene morphologies, which are consistent with the morphology phase diagram. In addition to confirming that carbon dimers are the dominant feeding species, we also find that the dominance level depends on the growth flux and temperature. Therefore, the proposed model is able to capture the growth kinetics, providing a useful tool for controlled synthesis of graphene with desired morphologies.

Keywords: graphene, kinetic Monte Carlo model, all atom, chemical vapor deposition, Cu(1 1 1) substrate

(Some figures may appear in colour only in the online journal)

1. Introduction

Graphene has attracted extensive interest for its fascinating lattice structures [1, 2] and excellent mechanical [3], electrical [4], thermal [5] or optical [6] properties. To realize its practical applications, controlled synthesis of large-scale, high-quality monolayer graphene with desirable morphology is a prerequisite. To date, monolayer graphene is typically synthesized either by liquid/mechanical exfoliation [7, 8] or by chemical vapor deposition (CVD) [9–15]. CVD growth of graphene is realized by the decomposition of carbon-containing gas molecules, typically methane or ethene, which is catalyzed by the substrate. There are a number of crystalline transition metals that have been utilized as catalytic substrates to grow graphene, including Ir(1 1 1) [9], Ru(0 0 0 1) [10], Cu(1 1 1) [11], Ni(1 1 1) [12], Au(1 1 1) [13], Pt(1 1 1) [14] and Rh(1 1 1) [15]. For the CVD growth of graphene, gas molecules are fed into the reactor to be decomposed to CH_x ($x = 0$–3) radicals [1]

[3] Author to whom any correspondence should be addressed.

at the initial stage, and these active carbon species are then dissolved and diffuse on the substrate. Some graphene nuclei can be formed by the diffusion and aggregation of these active species under suitable conditions. After the nucleation, these graphene nuclei further grow with the attachment of carbon species to the domain edges. The CVD always exhibits advantages in synthesis of large-scale and high-quality graphene with controllable size, domain morphologies and edge structures [9–15]. As a result, an in-depth understanding in the atomistic kinetics and morphology evolution during the CVD growth of graphene has become an important and fascinating research topic.

Significant theoretical efforts have been made to unveil the growth mechanisms of graphene [16], such as initial nucleations [17, 18], growth intermediates [19, 20], heterostructures [21, 22], edge structures [23, 24], and domain morphologies [25, 26] by using a variety of computational tools (*ab initio* calculations, molecular dynamics and kinetic Monte Carlo (kMC)). Among them, kMC method is able to provide a unique insight into the growth kinetics and underlying mechanisms at atomistic level with much larger time and length scale than other methods. In previous kMC simulations, graphene models were often constructed as a simple edge [26, 27] instead of a complete domain. In addition, the diffusion of adatoms on substrate surface was often considered implicitly, either by feeding carbon species with a concentration gradient [27] or by coupling the growth rate to a spatial distributed equation [28, 29]. Recently, all-atom kMC models have been proposed to simulate the growth of graphene domain by explicitly considering the diffusion of adatoms [30, 31]. We note, however, that these all-atoms kMC models either predicted a dendrite domain [30] or a compact graphene without six-fold symmetry [31]. So far, no one all-atom kMC model is able to predict all these different domain morphologies of graphene, indicating that some crucial atomistic events that dictate the graphene domain morphologies are missing in these kMC models.

It is well-known that a variety of graphene morphologies ranging from compact, to dendritic, and even to fragmentary shapes have been observed in experiments [9–15]. Such complex morphologies arise typically from non-equilibrium growth conditions, in which many important kinetic processes, such as diffusion of adatom on substrate surface, attachment of adatom to growing edge, and diffusion of atom along domain edge, have varying degree of influence, either coupled or competing, on the graphene morphology evolution. Currently, it remains unclear how many such critical events should be included and how these atomistic events are coupled or compete with each other to contribute to the evolution of domain morphology. Therefore, it is highly desirable to establish an all-atom kMC model by considering all the essential atomistic events to accurately predict the growth kinetics and morphological evolution of graphene domains.

In this work, we first construct an all-atom kMC model, aiming to study the growth kinetics of graphene and predict the domain morphology with energetic parameters from first-principles calculations [20]. Our simulations show that the constructed kMC model is able to predict many different graphene morphologies that were observed experimentally. Importantly, the simulation results are consistent with the qualitative phase diagram of the graphene morphologies in terms of the growth temperature and deposition flux. Beyond this, we also confirm that carbon dimers are the dominant feeding species for graphene growth. But the dimer concentration diminishes with decreasing the deposition flux or increasing the growth temperature. Hence, our kMC model not only correctly captures the growth mechanisms and kinetics of graphene during the CVD growth, but also provides useful guidelines for controllable synthesis of graphene with desired domain morphologies.

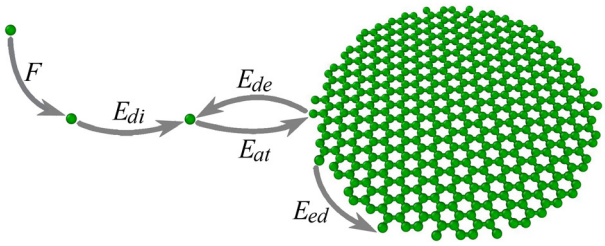

Figure 1. Schematic illustration of kMC simulation model. F represents the deposition flux. E_{di}, E_{at}, E_{de} and E_{ed} represent the energy barriers for the surface diffusion, attachment, detachment and edge diffusion processes, respectively.

2. Methods

Our kMC simulation model is illustrated in figure 1, in which 2D hexagonal graphene lattice (lattice constant $a = 2.46$ Å) grown on a Cu (1 1 1) substrate is used. An initial circular nucleus of graphene domain with a diameter of 4 nm is introduced at the center of the substrate surface. The dimensions of the simulation box are 213×246 Å^2, which consists of 20 000 sites. Starting from the nucleus, the growth kinetics of the domain is determined by the atomistic events considered in our kMC model (i.e. Gillespie algorithm [32]). At each given state, the kMC model specifies all the possible states that it can transit to at the next step based on the defined events. For example, the transition event from state i to state j, the occurrence rate for the event is calculated according to the transition state theory (TST) [33],

$$r_{i\to j} = \nu \exp(-\frac{E_{i\to j}}{k_b T}) \tag{1}$$

where, ν is the frequency of atomic vibration, which is taken as 1.0×10^{12} s^{-1} in our simulations [34], $E_{i\to j}$ is the energy barrier for the transition event, k_b is the Boltzmann constant, and T is the temperature.

The sum of all the rates gives rise to the total rate for escaping from the current state i, that is:

$$R_i = \sum_{j=1}^{n} r_{i\to j} \tag{2}$$

where, the deposition from the vapor phase to the substrate is also considered. The desorption from the substrate to vapor phase is not considered since it has a quite high energy barrier

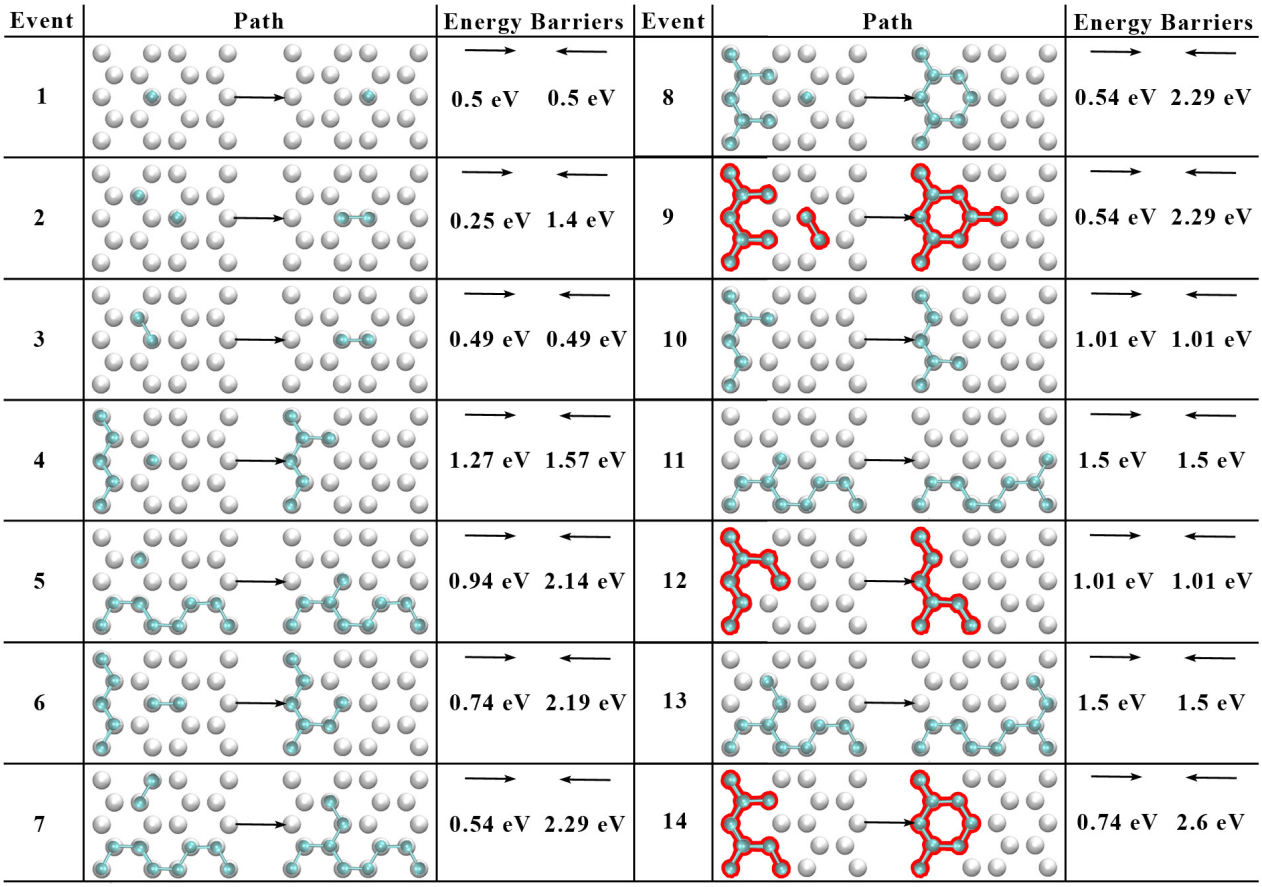

Figure 2. Atomistic events and the corresponding energetics in the kMC simulation model. White and light blue spheres represent the lattice sites and carbon atoms, respectively.

and thus is less probable to occur [35]. In order to determine which state j is to be selected for the transition from state i, a random number U_1 is generated within the range (0, 1). The state j that satisfies the following condition is selected,

$$\sum_{k=1}^{j-1} r_{i\to k} < U_1 \times R_i < \sum_{k=1}^{j} r_{i\to k}. \tag{3}$$

It is noted that the random number U_1 is utilized to choose an event to execute based on the occurrence rates of all events. The event with a higher occurrence rate (i.e. a lower energy barrier) has a higher probability to be chosen for execution. Meanwhile, the corresponding transition time can be calculated as

$$\Delta t = -\left(\frac{1}{R_i}\right) \ln U_2 \tag{4}$$

where, U_2 is another random number generated within the range (0, 1). Since the subsequently occurring events are highly dependent on the previous ones in kMC simulation, the code is difficult to implement in parallel and thus written as a serial program. The computational costs of the calculations are dependent on the deposition flux. For example, the cpu time increases from 72 core hours to 240 core hours with the deposition flux decreasing from 10 ML s^{-1} to 0.1 ML s^{-1}.

Wu *et al* reported that carbon dimers are the dominant feeding species for the epitaxial growth of graphene [20]. Therefore, in our kMC simulations, only carbon monomers and dimers are considered as the feeding species. The atomistic events for the growth kinetics involving the monomers and dimers and their corresponding energy barriers are defined and shown in figure 2. In particular, we consider the surface diffusion of a monomer (Event 1), the formation of a dimer with two monomers (Event 2), the surface diffusion of a dimer (Event 3), the attachment of a monomer to a zigzag edge (Event 4), the attachment of a monomer to an armchair edge (Event 5), the attachment of a dimer to a zigzag edge (Event 6), the attachment of a dimer to an armchair edge (Event 7), the attachment of a monomer to form a kink (Event 8), the attachment of a dimer to form a kink (Event 9), the edge diffusion of a monomer along a zigzag edge (Event 10), the edge diffusion of a monomer along an armchair edge (Event 11), the edge diffusion of a dimer along a zigzag edge (Event 12), the edge diffusion of a dimer along an armchair edge (Event 13), and the rotation of a dimer to form a kink (Event 14). All the energy barriers for the considered atomistic events are set according to Wu *et al*'s first-principles calculations [20], and therefore these parameters should be self-consistent. The crucial events that are essential for the formation of compact hexagonal graphene domains, but yet missing in previous kMC simulations [26–31] are highlighted in figure 2. Specifically, these are the attachment of a dimer to form a kink (Event 9), the diffusion of a dimer along the edge (Event 12), and the

rotation of a dimer to form a kink (Event 14). Event 6 (form a hexagonal ring) has the same energy barrier as Event 8 since the edges in both events will form the same pentagon by reconstruction [36] and the subsequent formation of hexagon is through the same monomer attachment process.

In our kMC simulations, carbon adatoms are deposited from the vapor phase to unoccupied sites on the substrate randomly (see figure 1). Both the starting species and those deposited at the substrate are carbon adatoms. After deposition, they can diffuse, form dimers and attach to the domain edge. The growth temperature in our kMC simulation is the temperature of carbon species at the substrate, corresponding to the furnace temperature in experiment. The rate of deposited adatom at the substrate depends on the deposition flux (see equation (2)), which is related to the gas pressure in experiment. During the simulation process, the substrate is fixed and the model is on-lattice, i.e. the activities of carbon species always follow the lattice of the substrate. In addition, the effect of the substrate on the graphene growth is also included in the energy barriers of atomistic events.

3. Results and discussion

3.1. Qualitative analysis on the factors that dictate graphene morphology

Before presenting the results of our kMC simulation, we carry out qualitative analyses on the factors that affect the graphene morphology during the epitaxial growth. The domain morphology of graphene is primarily determined by the rates of surface diffusion (r_{di}), attachment (r_{at}) and edge diffusion (r_{ed}), which in turn are controlled by their energetics (see E_{di}, E_{at}, E_{de}, E_{ed} in figures 1 and 2) and the growth parameters (F and T), where F and T are the deposition flux and growth temperature, respectively. The critical factor that dictates the domain morphology is the relative dominance between the attachment rate (r_{at}) and edge diffusion rate (r_{ed}). When $r_{at} \ll r_{ed}$, the graphene domain grows in the near thermodynamics-limited regime, in which a compact hexagonal shape with low-energy zigzag edges can be maintained due to the relatively fast edge diffusion rate and low attachment rate. Since the energy barrier for edge diffusion of a dimer is relatively high (1.01–1.5 eV), and that for attachment of a dimer is low (0.54–0.74 eV) (see figure 2), to obtain the compact hexagonal shape, one needs to have a high growth temperature to allow a sufficiently high edge diffusion rate, and a low deposition flux to enable a sufficiently low edge attachment rate [20]. Therefore, it is possible to achieve a compact hexagonal graphene with relatively high growth temperature and low deposition flux. For example, the growth temperature for graphene on Cu(1 1 1) and Cu(1 0 0) can be as high as 1025 °C [37], which is close to the melting temperature of Cu (1085 °C). A relatively low deposition flux can be achieved at the partial pressure ratio of CH_4:H_2 = 0.18:35 (Torr as their units) [37]. For Cu(1 1 1), when the ratio CH_4:H_2 is increased to 0.76:6.1, a relatively high deposition flux can be achieved, and as a result, the graphene morphology transforms from compact hexagon to fractal shape [37]. For Cu(1 0 0), the domain morphology transforms from compact shape to fractal one when the ratio CH_4:H_2 is increased to 0.73:35 [37]. With decreasing the growth temperature, the graphene domain may transform from compact hexagonal to circular shape. This is because when the growth temperature decreases, the edge diffusion of the attached atoms is limited and they cannot diffuse to the energetically favorable sites, resulting in a circular shape.

When $r_{at} >> r_{ed}$, the graphene domain grows in the near kinetics-limited regime, in which the domain morphology is governed by r_{at}/r_{di}, where r_{di} is the surface diffusion rate. When $r_{at} \ll r_{di}$, the surface diffusion is sufficiently fast to assist the adatoms to attach to the energetically favorable sites, and as a result, a compact hexagonal shape may also be achieved. However, it is not possible to achieve the compact hexagonal shape in this scenario for graphene growth on Cu(1 1 1). The underlying reason is that since the energy barrier for surface diffusion of a dimer is 0.49 eV, and that for attachment of a dimer is 0.54 eV, therefore, the surface diffusion rate is only comparable to the edge attachment rate, and thus it is not fast enough to achieve the compact shape (see figure 2) [20]. When $r_{at} >> r_{di}$, the graphene domain grows in the diffusion-limited regime, in which the domain morphology of graphene may become fractal. With increasing the deposition flux, the graphene domain may transform from a compact hexagonal to a fractal shape with six-fold symmetry. The underlying reason is that the increase of deposition flux increases the attachment rate. As a result, the surface diffusion and edge diffusion of the attached atoms are limited and they can only diffuse to the nearby energetically favorable sites, leading to the formation of rough edge morphologies with six-fold symmetry. If the growth temperature further decreases, the surface diffusion and edge diffusion of the attached atoms to the energetically favorable sites become even less probable due to the larger amount of attached atoms, thus resulting in a fractal shape without six-fold symmetry [20]. Our above analyses demonstrate a general frame of domain morphologies in the epitaxial growth of graphene. Below, we perform and discuss our kMC simulation results based on these analyses.

3.2. Morphological evolution and growth kinetics of different domain morphologies

The snapshots in the growth processes of different domain morphologies are shown in figures 3(a)–(d), in which the carbon monomers and dimers are not drawn in order to better show the morphology. When the growth temperature is 1000 °C and the deposition flux is 0.1 ML s^{-1}, the domain grows initially as a circular nucleus and transforms into a compact hexagonal shape due to the faster growth of armchair edges over the zigzag ones (see figure 3(a)). After that, the domain morphology retains a compact hexagonal shape. By converting the graphene domain to a circular shape with the same coverage, the growth rate is calculated with respect to the variation of radius with time, which is 0.24 μm min^{-1} at 1000 °C and 0.1 ML s^{-1}. When the growth temperature is kept at 1000 °C and the deposition flux increases to 10 ML s^{-1}, the domain morphology initially transforms from a circular shape into a compact hexagonal shape and then grows to a fractal one with

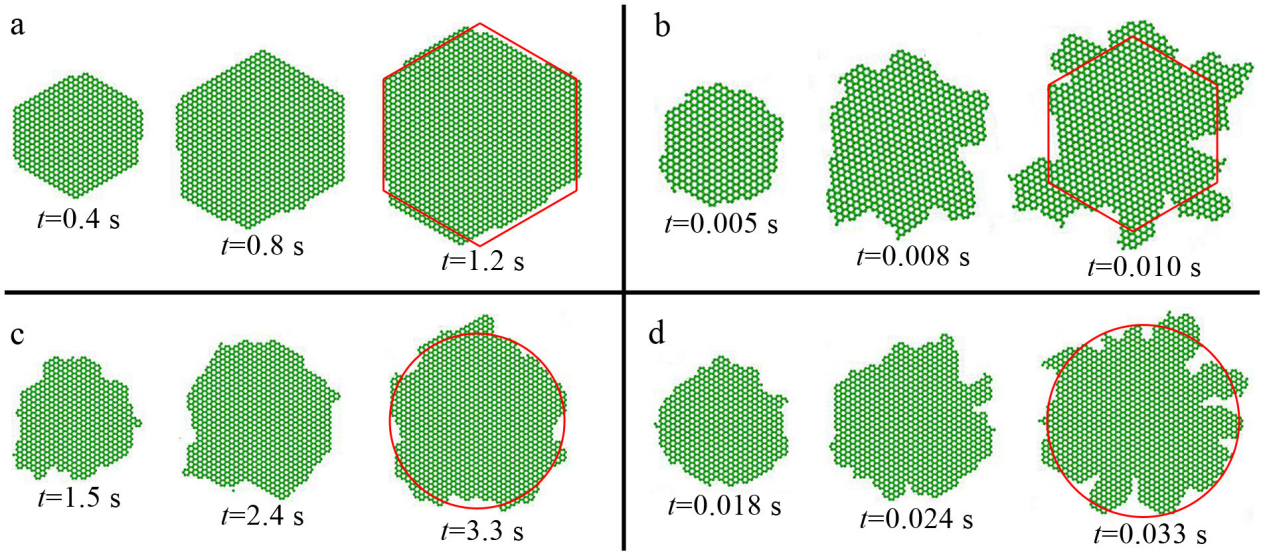

Figure 3. Morphological evolution of graphene domain for (a) hexagonal shape, (b) fractal shape with six-fold symmetry, (c) circular shape, and (d) fractal shape without six-fold symmetry.

six-fold symmetry due to the larger growth rate of the six corners in kinetic growth regime at a high growth temperature resulting from the increase of deposition flux (see figure 3(b)). Meanwhile, the growth rate for the domain radius increases from 0.24 μm min^{-1} to 23.64 μm min^{-1} with increasing the deposition flux from 0.1 ML s^{-1} to 10 ML s^{-1} at 1000 °C. Our previous work [38] only focused on the atomic events occurring at the growing edges (i.e. edge attachment and detachment) and did not consider the adatom diffusion on the substrate. Therefore, the previous model is only applicable to simulate the attachment-limited growth and the formation of compact shapes. However, the present work is an all-atom model, which considers the surface diffusion and dimer formation along with the edge attachment and detachment, and as a result, this all-atom model is also capable to simulate the diffusion-limited growth and the formation of dendrite domain morphologies.

The growth flux in our kMC model is defined as the C flux to the growth front. Our simulation results show that the graphene morphology transforms from a compact shape to a fractal shape with increasing the C flux. In Wu *et al*'s experiments [39], the transition from a compact shape to a fractal shape was achieved by decreasing the hydrogen partial pressure. In CVD of graphene, complex dehydrogenation processes occur. For hydrocarbon (CH_4) conversion to graphene on Cu substrate, in general, the following elementary steps take place [1]: (i) CH_4 adsorption on the metal substrate; (ii) CH_4 dehydrogenation, resulting in C species, such as CH_x ($x = 0$ to 3); (ii) surface diffusion of C species, and (iv) C attachment to the graphene domain edges and incorporation into the graphene lattice. Previous density functional theory calculations [1] revealed that the H-terminated graphene edges on Cu is energetically more favorable (i.e. more stable) than the bare graphene edges on Cu. As a result, H-termination at the edges makes C attachment more difficult at the edges, causing slow growth. Thus, to increase the growth rate, edge dehydrogenation (removing H from the edges) is needed. Since an increase in H_2 partial pressure will increase the H_2 flux, and a higher H_2 flux will lead to a higher level of H-termination at the graphene edges, as a result, there should be a slower C flux (slower C attachment and incorporation) at the edges, and a slower growth rate. It indicates that the observations in Wu *et al*'s experiments [39] are consistent with the present simulation results. Therefore, H-termination is implicitly considered in the C flux in present kMC model.

However, if the growth temperature decreases to 800 °C, while the deposition flux is relatively low at 0.1 ML s^{-1}, the domain maintains its circular shape due to the reduced edge diffusion rate at a lower attachment rate (see figure 3(c)). The corresponding growth rate for the domain radius decreases from 0.24 μm min^{-1} to 0.09 μm min^{-1} with decreasing the growth temperature from 1000 °C to 800 °C at 0.1 ML s^{-1}. When the growth temperature is kept at 800 °C and the deposition flux increases to 10 ML s^{-1}, the domain initially grows with a circular shape and then transforms into a fractal shape without six-fold symmetry, due to the enhanced rate of attachment and the limited surface and edge diffusion (see figure 3(d)). The corresponding growth rate for the domain radius increases from 0.09 μm min^{-1} to 7.94 μm min^{-1} with increasing the deposition flux from 0.1 ML s^{-1} to 10 ML s^{-1} at 800 °C. The temperature-induced morphological transition occurring in our simulations at 800 °C matches well with that occurring at 700 °C to 900 °C shown by theoretical analysis and experimental observation on Cu (1 1 1) [20, 40].

In order to further unveil the growth kinetics for the formation and maintenance of compact hexagonal, circular and fractal shape, the atomistic kinetics at the growing graphene edge is shown in figures 4(a)–(c). During the growth of compact hexagonal shape, the carbon monomers and dimers are attached to the zigzag edge initially to form a kink, generating energetically favorable armchair sites next to the kink (see figure 4(a)). Then, subsequently attached carbon monomers and dimers diffuse to the energetically favorable armchair sites, thus contributing to the kink propagation. These

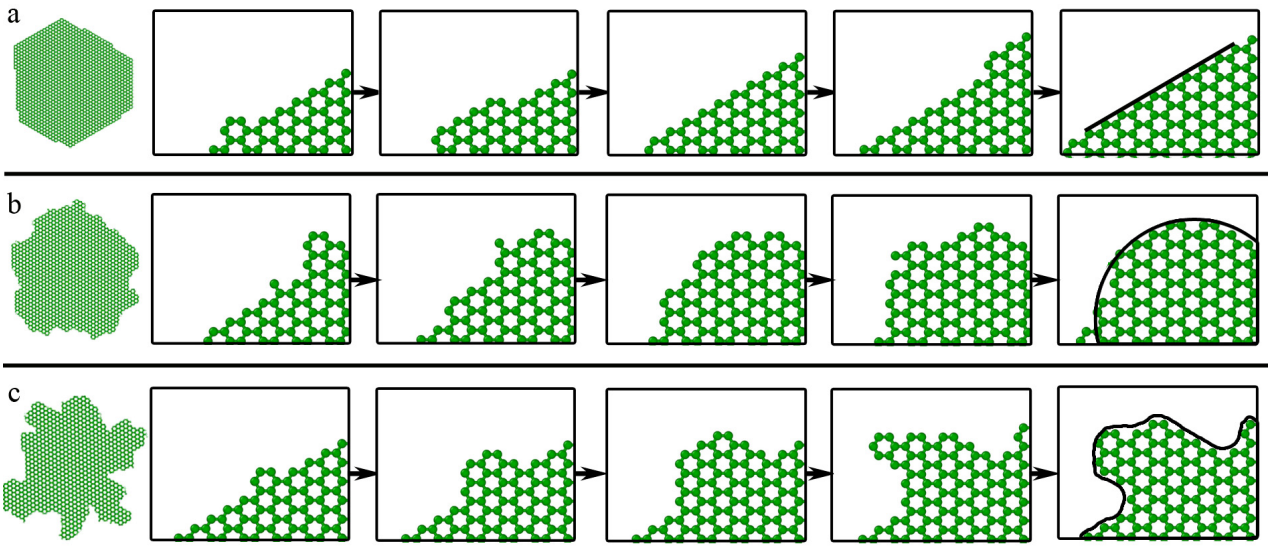

Figure 4. Atomistic kinetics at the edge during epitaxial growth of graphene domain with (a) a hexagonal shape, (b) a circular shape, and (c) a fractal shape.

armchair sites are quickly occupied by carbon atoms, forming a compact zigzag edge. After that, the next round of kink nucleation and propagation occurs at this newly formed zigzag edge. This repeating process leads to the formation and subsequent growth of the compact zigzag edge, resulting in the growth of compact hexagonal graphene. However, for the growth of circular shape, carbon monomer and dimer are attached to the zigzag and armchair sites equally due to large flux and limited surface diffusion and edge diffusion of carbon species (see figure 4(b)). When the flux further increases, the surface diffusion and edge diffusion of the attached atoms to the energetically favorable sites become even less probable due to the larger amount of attached atoms. Hence, the graphene domain acquires a fractal shape (see figure 4(c)).

3.3. Concentration of carbon dimers on Cu (1 1 1) surface during graphene growth

Wu *et al* [20] has performed accurate and detailed first-principles calculations to obtain the energetic data for the activities of carbon species on the Cu (1 1 1) substrate. Furthermore, Wu *et al* [20] has used kMC method with this set of energetic data to estimate the concentrations of carbon species on the substrate. Their study has demonstrated the dominance of dimers, and presence of a clear carbon concentration gradient, which is confirmed by previous experimental observation [40]. In the following, we examine the concentration of carbon dimers on Cu (1 1 1) substrate surface, which is the ratio of dimers to the total carbon species. The coverage is the ratio of domain area to the model size, which increases with the graphene domain growth. The concentration of carbon dimers on Cu (1 1 1) surface at the same growth temperature ($T = 800$ °C) and different deposition fluxes ($F = 10$ ML s^{-1}, 1 ML s^{-1} and 0.1 ML s^{-1}) are shown in figure 5(a). The results indicate that carbon dimers are indeed the dominant feeding species during the epitaxial growth of graphene at different deposition fluxes. However, the dimer concentration decreases from ~94% to ~50% with the deposition flux decreasing from 10 ML s^{-1} to 0.1 ML s^{-1}. The underlying reason is that the quantity of carbon monomers decreases with decreasing the deposition flux, resulting in a lower probability to meet to form carbon dimers.

The concentration of carbon dimers on Cu (1 1 1) surface at the same deposition fluxes ($F = 1$ ML s^{-1}) and different growth temperature ($T = 600$ °C, 800 °C and 1000 °C) are also calculated and shown in figure 5(b). The results indicate that the dimer concentration decreases from ~92% to ~51% with increasing the growth temperature from 600 °C to 1000 °C, further confirming that carbon dimers are the dominant growth species [20]. Based on the occurrence rate calculated by the TST (see equation (1)), the increase of the growth temperature enhances the event probabilities of adatoms on the substrate, which become relatively dominant in comparison to the deposition event. Therefore, the effect of temperature increase is similar to that of deposition flux decrease, resulting in the decrease of monomer quantity on the substrate. The decrease of monomer quantity further decreases the probability of monomers to form carbon dimers, resulting in the decrease of dimer concentration.

3.4. Adaptation of this kMC model to epitaxial growth of other 2D materials

In kMC simulations, the growth kinetics of the domain is determined by the defined atomistic events. Therefore, the accuracy of kMC simulation is dependent on the detailed consideration of dominant events and the precision of corresponding energetic parameters, which can be obtained by first-principles calculations. Here, we have included additional three important events (i.e. the edge attachment of carbon species to form a kink, the diffusion of carbon species along the edge, and the rotation of dimers to form kinks) on top of previous kMC simulation [30, 31], which only consider the usual atomistic events (i.e. the surface diffusion, the attachment to zigzag

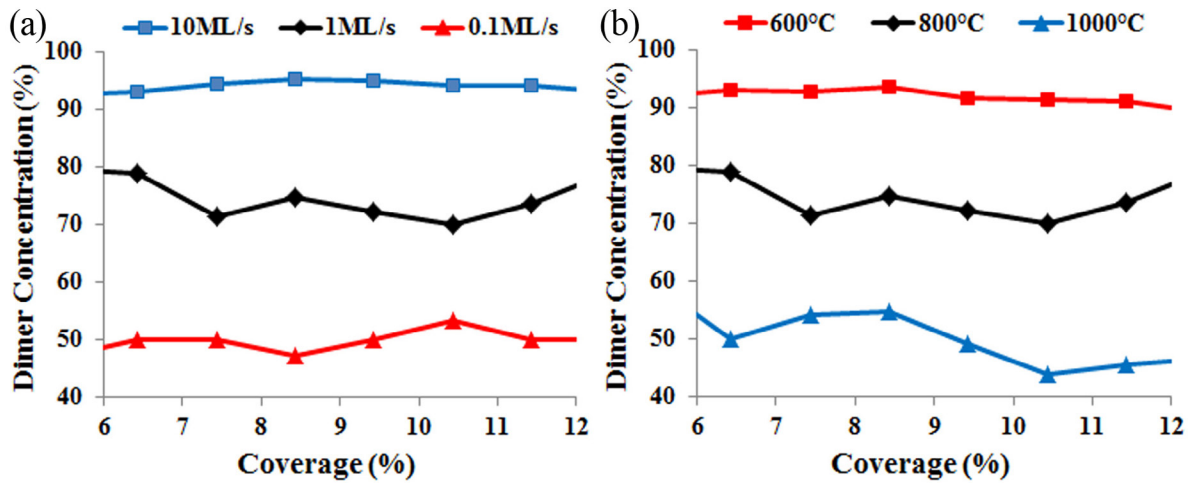

Figure 5. Concentration of carbon dimers on Cu (1 1 1) surface during graphene growth (a) at the same growth temperature ($T = 800$ °C) and different deposition fluxes ($F = 10$ ML s^{-1}, 1 ML s^{-1} and 0.1 ML s^{-1}), and (b) at the same deposition flux ($F = 1$ ML s^{-1}) and different growth temperatures ($T = 600$ °C, 800 °C and 1000 °C). The coverage is the ratio of domain area to the model size, which increases with the graphene domain growing.

edge, the attachment to armchair edge and so on). Therefore, by considering these additional events with accurate energetic parameters from first-principles calculations [20], our all-atom kMC model can successfully simulate the epitaxial growth of graphene under different growth temperatures and deposition fluxes, and the simulation results match well with previous experimental observations [39, 40]. Different forms of the evolving substrate and factors (growth temperature and deposition flux) affect the feeding species and growing morphology, which is similar to the reported general patterns of interface growth [41].

For the epitaxial growth of other 2D materials, there are several similarities in comparison with graphene. For example, the growths of TMDs are also via the initial deposition of adatoms to the substrate and subsequent diffusion and attachment to the growing edge. Therefore, our kMC model is also applicable to simulate other 2D materials with modifications to corresponding lattice structures and energetic data. We have already adapted this model to simulate the growth of monolayer WSe_2 on Au (1 1 1) surface under different growth temperatures and deposition fluxes [42], whose domain morphology and growth rate are in good agreement with experimental observations [43]. Besides, this model is also applicable to simulate the growth of multi-layer MoS_2 by considering the adatom concentration and edge attachment contributing to the growth of each layer [44].

However, there are still some major differences between the graphene model and TMD model. For graphene, the dominant species contributing to the growth are carbon dimers. Therefore, the formation of dimers on the substrate, the attachment of dimers to the edge, and the rotation of dimers at the edge need to be included. For TMDs, the feeding species are transition metal adatoms and chalcogen adatoms, whose deposition fluxes, surface diffusions and edge attachments need to be treated separately. Besides, the corresponding energetic data for graphene and TMDs are quite different, depending on the feeding species and growth substrate. The graphene model developed here provides a useful tool to predict the growth of graphene, which also paves the way to study the multi-layer graphene, multi-grain graphene and graphene/TMD heterostructure growth in the future.

4. Conclusions

In this work, we formulated a kMC model to study the evolution of graphene domain morphology during epitaxial growth. We first qualitatively analyzed the main factors that controlled the growth morphology and proposed a phase diagram for the graphene morphologies in terms of the growth temperature and deposition flux. Our kMC simulations demonstrated that the initially circular graphene morphology transformed into a compact hexagonal one, and then into a fractal domain with six-fold symmetry with an increase in the deposition flux at a fixed high temperature. However, when the growth temperature is low, the hexagonal graphene morphology with a six-fold symmetry is lost and transitioned to a circular shape at a low deposition flux. It transformed into a fractal shape without six-fold symmetry when the deposition flux is increased furthermore. In addition, we confirmed that carbon dimers were the dominant feeding species for the epitaxial growth of graphene, but the dimer concentration decreased with decreasing the deposition flux or increasing the growth temperature. Hence, our kMC model, which includes the essential atomistic events, is able to capture the underlying growth mechanism and kinetics of graphene growth, and its predictions may provide valuable guidelines for experimental fabrication of graphene with desired domain morphology.

Acknowledgments

The authors gratefully acknowledge support from the Science and Engineering Research Council through grant (152-70-00017) and use of computing resources at the A∗STAR

Computational Resource Centre and National Supercomputer Centre, Singapore.

Notes

The authors have no competing interest to declare.

ORCID iDs

Shuai Chen https://orcid.org/0000-0001-9455-6015
Gang Zhang https://orcid.org/0000-0001-9812-8106
Viacheslav Sorkin https://orcid.org/0000-0001-8284-5354

References

[1] Hao Y *et al* 2013 The role of surface oxygen in the growth of large single-crystal graphene on copper *Science* **342** 720–3
[2] Rizzo D J, Veber G, Cao T, Bronner C, Chen T, Zhao F, Rodriguez H, Louie S G, Crommie M F and Fischer F R 2018 Topological band engineering of graphene nanoribbons *Nature* **560** 204–8
[3] Melios C, Giusca C E, Panchal V and Kazakova O 2018 Water on graphene: review of recent progress *2D Mater.* **5** 022001
[4] Zhou X, Ji S-H, Chockalingam S P, Hannon J B, Tromp R M, Heinz T F, Pasupathy A N and Ross F M 2018 Electrical transport across grain boundaries in graphene monolayers on SiC(0 0 0 1) *2D Mater.* **5** 031004
[5] Zhang G and Zhang Y W 2017 Thermal properties of two-dimensional materials *Chin. Phys.* B **26** 034401
[6] Zhu C, Du D and Lin Y 2015 Graphene and graphene-like 2D materials for optical biosensing and bioimaging: a review *2D Mater.* **2** 032004
[7] Nicolosi V, Chhowalla M, Kanatzidis M G, Strano M S and Coleman J N 2013 Liquid exfoliation of layered materials *Science* **340** 1226419
[8] Yi M and Shen Z A 2015 Review on mechanical exfoliation for the scalable production of graphene *J. Mater. Chem.* A **3** 11700–15
[9] Coraux J, N'Diaye A T, Engler M, Busse C, Wall D, Buckanie N, zu Heringdorf F J M, van Gastel R, Poelsema B and Michely T 2009 Growth of graphene on Ir(1 1 1) *New J. Phys.* **11** 023006
[10] Loginova E, Bartelt N C, Feibelman P J and McCarty K F 2009 Factors influencing graphene growth on metal surfaces *New J. Phys.* **11** 063046
[11] Gao L, Guest J R and Guisinger N P 2010 Epitaxial graphene on Cu(1 1 1) *Nano Lett.* **10** 3512–6
[12] Yamamoto K, Fukushima M, Osaka T and Oshima C 1992 Charge-transfer mechanism for the monolayer graphite)/ Ni(1 1 1) system *Phys. Rev.* B **45** 11358
[13] Nie S, Bartelt N C, Wofford J M, Dubon O D, McCarty K F and Thürmer K 2012 Scanning tunneling microscopy study of graphene on Au(1 1 1): growth mechanisms and substrate interactions *Phys. Rev.* B **85** 205406
[14] Preobrajenski A B, Ng M L, Vinogradov A S and Mårtensson N 2008 Controlling graphene corrugation on lattice-mismatched substrates *Phys. Rev.* B **78** 073401
[15] Voloshina E N, Dedkov Y S, Torbrügge S, Thissen A and Fonin M 2012 Graphene on Rh(1 1 1): scanning tunneling and atomic force microscopies studies *Appl. Phys. Lett.* **100** 241606
[16] Gao J, Xu Z, Chen S, Bharathi M S and Zhang Y-W 2018 Computational understanding of the growth of 2D materials *Adv. Theory Simul.* **1** 1800085
[17] Gao J, Yip J, Zhao J, Yakobson B I and Ding F 2011 Graphene Nucleation on transition metal surface: structure transformation and role of the metal step edge *J. Am. Chem. Soc.* **133** 5009–15
[18] Yuan Q, Gao J, Shu H, Zhao J, Chen X and Ding F 2012 Magic carbon clusters in the chemical vapor deposition growth of graphene *J. Am. Chem. Soc.* **134** 2970–5
[19] Bharathi M S, Hao Y, Ramanarayan H, Rywkin S, Hone J C, Colombo L, Ruoff R S and Zhang Y-W 2018 Oxygen-promoted chemical vapor deposition of graphene on copper: a combined modeling and experimental study *ACS Nano* **12** 9372–80
[20] Wu P, Zhang Y, Cui P, Li Z, Yang J and Zhang Z 2015 Carbon dimers as the dominant feeding species in epitaxial growth and morphological phase transition of graphene on different Cu substrates *Phys. Rev. Lett.* **114** 216102
[21] Lee H W, Jung H, Yeo B C, Kim D and Han S S 2018 Atomistic sodiation mechanism of a phosphorene/ graphene heterostructure for sodium-ion batteries determined by first-principles calculations *J. Phys. Chem.* C **122** 20653–60
[22] Zhang Y, Pei Q X, Wang C M, Yang C and Zhang Y W 2018 Interfacial thermal conductance and thermal rectification of hexagonal BC_nN/graphene in-plane heterojunctions *J. Phys. Chem.* C **122** 22783–9
[23] Gao J, Zhao J and Ding F 2012 Transition metal surface passivation induced graphene edge reconstruction *J. Am. Chem. Soc.* **134** 6204–9
[24] Artyukhov V I, Liu Y and Yakobson B I 2012 Equilibrium at the edge and atomistic mechanisms of graphene growth *Proc. Natl Acad. Sci. USA* **109** 15136–40
[25] Luo Z, Kim S, Kawamoto N, Rappe A M and Johnson A C 2011 Growth mechanism of hexagonal-shape graphene flakes with zigzag edges *ACS Nano* **5** 9154–60
[26] Jiang H and Hou Z 2015 Large-scale epitaxial growth kinetics of graphene: a kinetic Monte Carlo study *J. Chem. Phys.* **143** 084109
[27] Wu P, Jiang H, Zhang W, Li Z, Hou Z and Yang J 2012 Lattice mismatch induced nonlinear growth of graphene *J. Am. Chem. Soc.* **134** 6045–51
[28] Chen S, Gao J, Bharathi M S, Zhang G, Sorkin V, Ramanarayan H and Zhang Y-W 2019 Unveiling the competitive role of etching in graphene growth during chemical vapor deposition *2D Mater.* **6** 015031
[29] Fan L, Zou J, Li Z, Li X, Wang K, Wei J, Zhong M, Wu D, Xu Z and Zhu H 2012 Topology evolution of graphene in chemical vapor deposition, a combined theoretical/ experimental approach toward shape control of graphene domains *Nanotechnology* **23** 115605
[30] Gaillard P, Chanier T, Henrard L, Moskovkin P and Lucas S 2015 Multiscale simulations of the early stages of the growth of graphene on copper *Surf. Sci.* **637** 11–8
[31] Taioli S 2014 Computational study of graphene growth on copper by first-principles and kinetic Monte Carlo calculations *J. Mol. Model.* **20** 2260
[32] Gillespie D T 1977 Exact stochastic simulation of coupled chemical reactions *J. Phys. Chem.* **81** 2340–61
[33] Nitzan A 2006 *Chemical Dynamics in Condensed Phases: Relaxation, Transfer and Reactions in Condensed Molecular Systems* (New York: Oxford University Press)
[34] Voter A F 2007 Introduction to the kinetic Monte Carlo method *Radiat. Eff. Solids* **235** 1–23
[35] Nie Y, Liang C, Zhang K, Zhao R, Eichfeld S M, Cha P R, Colombo L, Robinson J A, Wallace R M and Cho K 2016 First principles kinetic Monte Carlo study on the growth patterns of WSe_2 monolayer *2D Mater.* **3** 025029
[36] Shu H, Chen X, Tao X and Ding F 2012 Edge structural stability and kinetics of graphene chemical vapor deposition growth *ACS Nano* **6** 3243–50

[37] Jacobberger R M and Arnold M S 2013 Graphene growth dynamics on epitaxial copper thin films *Chem. Mater.* **25** 871–7
[38] Chen S, Gao J, Bharathi M S, Zhang G, Sorkin V, Ramanarayan H and Zhang Y-W 2019 A kinetic Monte Carlo model for the growth and etching of graphene during chemical vapor deposition *Carbon* **146** 399–405
[39] Wu B, Geng D, Xu Z, Guo Y, Huang L, Xue Y, Chen J, Yu G and Liu Y 2013 Self-organized graphene crystal patterns *NPG Asia Mater.* **5** e36
[40] Nie S, Wofford J M, Bartelt N C, Dubon O D and McCarty K F 2011 Origin of the Mosaicity in graphene grown on Cu(1 1 1) *Phys. Rev.* B **84** 155425
[41] Barabási A L and Stanley H E 1995 *Fractal Concepts in Surface Growth* (Cambridge: Cambridge University Press)
[42] Chen S, Gao J, Bharathi M S, Zhang G, Sorkin V, Ramanarayan H and Zhang Y-W 2019 Origin for the ultrafast growth of monolayer WSe2 via chemical vapor deposition *npj Comput. Mater.* **5** 28
[43] Gao Y *et al* 2017 Ultrafast growth of high-quality monolayer WSe_2 on Au *Adv. Mater.* **29** 1700990
[44] Chen S, Gao J, Bharathi M S and Zhang Y-W 2019 A kinetic Monte Carlo study for mono- and bi-layer growth of MoS_2 during chemical vapor deposition *Acta Phys. -Chim. Sin.* **35** 1119–27